Carbohydrate Polymers 114 (2014) 514–520

Contents lists available at ScienceDirect

Carbohydrate Polymers

journal homepage: www.elsevier.com/locate/carbpol

Adsorption of molybdate on molybdate-imprinted chitosan/triethanolamine gel beads

Liang Zhang [a,*], Juanqin Xue [b], Xingwen Zhou [c], Xiang Fei [a], Yang Wang [a], Yuanzhen Zhou [a], Lvling Zhong [a], Xuanli Han [a]

[a] College of Science, Xi'an University of Architecture and Technology, Xi'an, Shaanxi, 710055, China
[b] College of Metallurgy Engineering, Xi'an University of Architecture and Technology, Xi'an, Shaanxi, 710055, China
[c] Technical Center of Jin Dui Cheng Molybdenum Co., Ltd, Xi'an, Shaanxi, 710077, China

ARTICLE INFO

Article history:
Received 28 May 2014
Received in revised form 11 August 2014
Accepted 11 August 2014
Available online 27 August 2014

Keywords:
Chitosan
Ion-imprinted technology
Molybdate
Triethanolamine
Adsorption

ABSTRACT

Mo (VI)-imprinted chitosan (CTS)/triethanolamine (TEA) gel beads (Mo (VI)-ICTGBs) (ICTGBs = imprinted chitosan triethanolamine gel beads) were prepared by using ion-imprinted technology, in which TEA and molybdate solution were used in coagulation bath. The spectrum of FT-IR implies that bonding are formed between TEA and the primary hydroxyl of CTS, and ion gel reaction happen between CTS and molybdate; XRD patterns also prove the change among CTS, TEA and molybdate. SEM images and N_2 adsorption show that the surface area increases obviously after eluting Mo (VI) ions. The adsorption isotherm of Mo (VI)-ICTGBs imply that the adsorption process is according with Freundlich model. Adsorption kinetics suggests that the pseudo-second order adsorption mechanism is predominant for this adsorbent system of Mo (VI)-ICTGBs. The Mo (VI)-ICTGBs show high adsorption capacity and good selectivity for Mo (VI) anions in the coexistence system at pH = 6.0. The Mo (VI)-ICTGBs have a good application prospect, because it is with a simple and rapid technique and good durance.

1. Introduction

The recycling of Mo becomes very important due to the increasing demand for Mo in the industrial field. Many technologies have been applied in the recycling field of Mo at present, i.e. biological, chemical and physical treatments. Adsorption is a simple and facile technique used in molybdate treatment. Different adsorbents, such as pyrite, synthetic schwertmannite, kaolinite, organo-bentonite, goethite, natrolite, titania, iron oxide, and aluminum oxide, have been used for molybdate removal from aqueous solutions (Antelo et al., 2012; Atia, 2008; Xu and Washington, 2006). In addition, new adsorbing materials, including resins, solvent-impregnated resins (Atia, 2008), carbon base materials (Afkhami and Conway, 2002; Namasivayam and Sangeetha, 2006) or biomass, have attracted some interest. Removal and preconcentration of Mo (VI) from water and wastewater solutions has been investigated using carminic acid modified anion exchanger (Asem, Ahmed, & Haytham, 2008). Magnetic resins derived from glycidyl methacrylate and croslinked with divinylbenzen or *N*,*N*-methylenebisacrylamide have been also prepared (Rojas et al., 2005). However, the above treatment for Mo is not recycling, but rather removal. Therefore, in order to reach the aim of recycling for Mo, the selective adsorption for molybdate is necessary.

CTS is a well-known biopolymer, whose high nitrogen content confers not only remarkable ability for the sorption of metal ions from dilute effluents, but also the sorption of metal anions from dilute effluents (Vold et al., 2003; Muzzarelli, 2011). CTS have been used for removing Cr (VI), arsenic, Mo (VI), etc. (Chassary, Vincent, & Guibal, 2004; Dambies, Vincent, Domard, & Guibal, 2001; Guibal, Milot, & Tobin, 1998; Guibal, Milot, & Roussy, 2000; Muzzarelli & Rocchetti, 1973). The study also shows that CTS is effective for removing molybdate with high sorption capacities (Guibal et al, 1998, 2000). Some researchers have further proved that the gel bead could be formed self-rembulately by CTS and Molybdate (Dambies et al., 2001; Draget, Värum, Moen, Gynnild, & Smidsrød, 1992). This new gel technique leads to a structure different from that produced during alkaline coagulation of a CTS solution. According to the self-rembulate propriety of CTS solution and Molybdate, the crosslinking CTS has been prepared by ion gel reaction. The ion gel of CTS formed by CTS and molybdate is suitable for adsorbing other anions, such as As (V) (Chen et al., 2008; Dambies, Vincent, & Guibal, 2002). The above CTS material is still shortcoming in specific and reusability. Some researchers have prepared crosslinked metal complexed CTS by using a metal ion as template, and then removed

* Corresponding author. Tel.: +86 2982201469.
E-mail address: zl98zl@hotmail.com (L. Zhang).

http://dx.doi.org/10.1016/j.carbpol.2014.08.049
0144-8617/

the template ion to overcome the above problem. The resins have good selectivity and show maximum adsorption capacity (Varma, Deshpande, & Kennedy, 2004). When the ion imprinted technology was applied for the ion gel formed by CTS and molybdate by using molybdate anion as template, the imprinted material became powder and a loss after eluting molybdate from the ion gel. Therefore, it is necessary to add a crosslinking agent for the stability of the Mo (VI) imprinted material. Zhang et al. have reported that TEA has coagulating function for CTS solution (Zhang et al., 2012). The similar study also shows that amino functions are involved in the sorption mechanisms, together with carbonyl sites in adsorption anion (Guibal, Milot, Eterradoss, Gauffier. & Domard, 1999). So TEA is a suitable coagulating agent for forming the imprinted material considering adding adsorption site and stability of gel.

The subject of this work is to prepare Mo (VI)-ICTGB by ion imprinted technique and ion gel reaction between CTS and molybdate, and utilizing the material for selective adsorption of Mo (VI). SEM and N_2 adsorption, FT-IR and XRD were used to characterize the material to study the mechanism of forming gel beads. Static equilibrium and kinetics were performed to explore adsorption mechanism of the material. The Mo (VI)-ICTGB were applied into a mixed solution containing molybdate, chromate, vanadate and arsenate was used to perform a study of competitive adsorption in this work. The Mo (VI)-ICTGB were applied to the factual wastewater.

2. Materials and methods

2.1. Materials

All reagents used in this work were of analytic grade. Chitosan (CTS, ≥90% deacetylation) were purchased from Sinopharm Chemical Reagent Co. Ltd. Ammonium molybdate were obtained from Shanghai ShenBo Chemical Co. Ltd. Triethanolamine (TEA) were obtained from Tianjin Tianli Chemical Reagent Co. Ltd. Other chemicals were purchased from Xi'an Chemical Reagent Factory.

2.2. Analytical instrumentation

IR Fourier transform infrared spectrometer (FT-IR, Shimadzu. co., Japan) was used to characterize and analyze the forming mechanism of the composite beads. X-ray diffraction (XRD) analysis was carried out by a PerkinElmer PHI-5400 diffract meter, employing Cu Kα radiation of wavelength 1.54. The data were taken in the range of 3–90° (2θ), with a step size of 0.02°. The N_2 adsorption–desorption isotherms were measured at −196 °C using a Micromeritics ASAP 2020-Physisorption Analyzer. Prior to the characterization, samples were degassed for 5 h at 100 °C. The specific surface area was calculated according to the BET (Brunauer–Emmet and Teller) model, while the pore size and pore volume were calculated using the Barrett–Joyner–Halenda (BJH) formula. The surface morphology of the bead was examined using FEI Quanta 200 scanning electron microscope (SEM). The absorbance of Mo (VI) was detected by GFS97 graphite furnace atomic absorption spectrophotometer (GFAAS, Thermo co., USA).

2.3. Preparation of Mo (VI)-ICTGB

The process of preparing Mo (VI)-ICTGBs has been described by Fei, Zhang, Zhong, Chen, and Ma (2012), and a flow chart of the preparation of Mo (VI)-ICTGB was shown in Fig. S1 (seen in Supporting Information). CTS-acetate solution was prepared by dissolving the powder of CTS (0.20 g) in 10.0 mL of 2% (v/v) acetic acid at room-temperature till the solution became homogeneous. After deaeration, the casting solution was slowly dropped into 200 mL of 11% (v/v) of TEA with syringe (needle, Φ0.4 mm), and stirred for 4 h to form the non-imprinted CTS/TEA gel beads. After being washed and dried, the beads were labeled as NICTGBs (non imprinted CTS/TEA gel beads). According to the same procedure, the casting solution was dropped into 200 mL of ammonium molybdate solution (8.0 g L^{-1}) to form the CTS/Mo (VI) beads (labeled as CMoBs). The CTS/TEA/Mo (VI) beads (CTMoBs) were prepared by the same procedure in the mixed solution of 11% (v/v) of TEA and ammonium molybdate solution (8.0 g L^{-1}).

The CTMoBs were soaked and stirred in 50 mL of 8.0 g L^{-1} NaOH solution about 1.5 h to remove Mo (VI) ions, and the procedure was performed for three times. The Mo (VI)-ICTGBs were obtained by rinsing repeatedly with deionized water. The Mo (VI)-ICTGBs (Φ1-1.5 mm) were soaked in deionized water.

2.4. Adsorption capacity testing

All the adsorption experiments were carried out at room-temperature. Adsorbent concentration was kept constant at 0.0400 g in 20.00 mL solution, and the initial pH of solution was adjusted to 6.0 with 0.1 M sulphuric acid. The concentration of Mo (VI) in the filtrate and initial concentration were determined by using GFAAS. Adsorption capacity could be calculated by Eq. (1) (Ren et al., 2013; Vold, Vårum, Guibal, & Smidsrød, 2003).

$$Q = (C_0 - C) \times V/m \quad (1)$$

Where Q is the adsorption capacity (mg g^{-1}); C_0 and C are the initial and equilibrium concentrations of Mo (VI) (mg L^{-1}), respectively; m is the dry mass of Mo (VI)-ICTGBs (g); V is the volume of adsorption solution (L).

2.5. Adsorption selectivity experiments

The mixed solution (100.0 mg L^{-1} for each element) prepared by solving molybdate, chromate vanadate and arsenate was used to perform an experiment of competitive adsorption. Cr (VI), As (V) and V (VI) ions were chosen as similar anions to prove the specificity of Mo (VI)-ICTGBs for Mo (VI) in this work. The concentration of each ion in the remaining solution was measured with GFAAS after adsorption equilibrium. Distribution coefficients (K_d) of Cr (VI) ion, As (V) ion and V (VI) ion with respect to Mo (VI) were calculated by Eq. (2) (Ren et al., 2008; Naja & Volesky, 2011).

$$K_d = Q_e/C_e \quad (2)$$

Where K_d is the distribution coefficient; Q_e is the equilibrium adsorption capacity of metal ions (mg g^{-1}); C_e is the equilibrium concentrations of metal ions (mg L^{-1}).

Selectivity coefficient (k) for the binding of Mo (VI) in the presence of competitor species can be calculated by Eq. (3).

$$k = K_{\text{template metal}}/K_{\text{interferent metal}} \quad (3)$$

2.6. Column adsorption studies

Column flow adsorption experiments were performed in a glass column of about 1.2 cm internal diameter and 25 cm length. The column was filled with Mo (VI)-ICTGBs (Φ1–1.5 mm). The Mo (VI) ion solution (100 mg L^{-1}) was allowed to flow through the column at a constant flow rate (2 mL min^{-1}) throughout the experiment. The pH of the inlet solution was adjusted to 6.0 at the start of the experiment. The effluent solution was collected at 5 min intervals and the concentration of Mo (VI) ion in the effluent solution was monitored by GFAAS. The solutions were diluted to detection range for Mo (VI) prior to analysis.

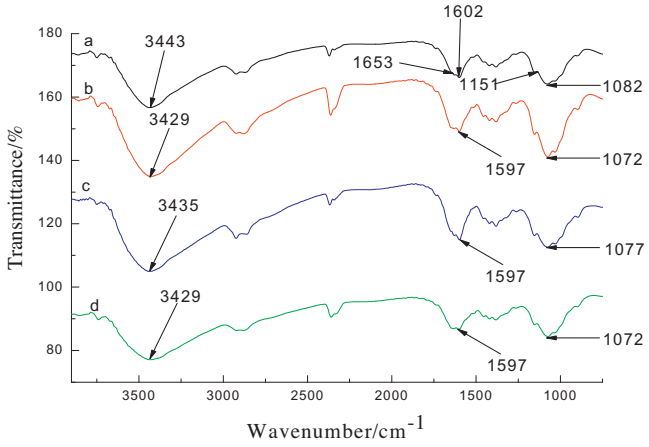

Fig. 1. FT-IR spectra of (a), CTS; (b), NICTGB; (c), CTMoB; (d)Mo (VI)-ICTGB.

3. Results and discussion

3.1. Effect of TEA concentration in the mixed coagulation

Some parameters in the preparation of Mo (VI)-ICTGB, including CTS concentration, Mo(VI) concentration, solidification temperature and eluent, have been discussed by Fei et al. (2012). In this work, the mixed coagulation bath containing TEA and molybdate was used in the process of forming gel beads. TEA could react with CTS by hydrogen bond (Zhang et al., 2012). The adsorption capacity of gel beads for Mo (VI) is best at 11% of TEA (the data is shown in Fig. S2, Supporting Information). In fact, the pH value of the mixed solution increases with increasing the ratio of TEA because it is an organic weak base. The pH value in the mixed coagulation bath is about 6.0 when TEA is up to 11%. The distribution of molybdate ion species is affected by the pH of solution (Dambies et al., 2001). The major molybdate species is MoO_4^{2-} in the mixed coagulation bath at pH = 6.0. Therefore, the gel beads are formed by the action among CTS, $MoO_4^{2-}$and TEA. When TEA is above 11%, the adsorption capacity of Mo (VI)-ICTGBs decreases with increasing pH. This may be due to the change from the ionic gel (MoO_4^{2-}) to alkaline gel (OH^-), which cause the failure of preparing ion imprinted Mo (VI).

3.2. FT-IR analysis

The shapes of most peaks in Fig. 1 were similar. The major peaks of the CTS are located around 3443 cm^{-1} (O—H and N—H stretching vibration), 1602 cm^{-1} for N-H deformation vibration (Wei, Sun, Qian, Ye, & Ma, 2009), 1082 and 1022 cm^{-1} (C—OH stretching vibration).

The major peaks in Fig. 1b corresponding to CTS were shifted to 3429 cm^{-1}, 1597 cm^{-1}, 1072 cm^{-1}, respectively. These changes could be attributed to a hydrogen bond interaction between TEA and CTS (Zhang et al., 2012). Comparing Fig. 1b and Fig. 1c, the peak at 3429 cm^{-1} was shifted to 3435 cm^{-1}, the peak at 1072 cm^{-1} was shifted to 1077 cm^{-1}. There is no peak at 1520 cm^{-1} corresponding to $—NH_3^+$ shown in the beads prepared by molybdate solution (Lee et al., 2001). This indicates that the process of forming gel beads is not only controlled by molybdate ionic crosslinking, but a cooperative action of TEA and molybdate containing hydrogen bond and ionic crosslinking. For Mo (VI)-ICTGB, these peaks were back to the same position with the peaks in NICTGB. This implies that the action in Mo (VI)-ICTGB after eluting Mo (VI) is the same with that in NICTGB.

3.3. Characterization of CTS gel beads by SEM and N_2 adsorption

Fig. 2a shows the dried Mo (VI)-ICTGBs (100 ×) with near-spherical shape, and these beads is less than 1 mm in diameter. Fig. 2b shows the surface appearance of CTS gel beads prepared in TEA solutions. The surface of the NICTGB is flat and dense. There is a fingerprint for CMoB in Fig. 2c, which may be due to ionic gel reaction between molybdate and CTS among Linear polymer structure of CTS. A surface appearance combining the two surface appearances of NICTGB and CMoB is shown in Fig. 2d, which implies the reaction among CTS, TEA and molybdate. The CTMoBs become smaller and denser compared to the material coagulated in sodium hydroxide solutions. This is in agreement with the results obtained by Dambies et al. (2001). Compared with CTMoB, Mo (VI)-ICTGB has a rough and bumpy surface in Fig. 2e, which shows the increasing of specific surface area compared to CTMoB. The increasing of specific surface area has been proved by the results obtained by N_2 adsorption. Compared with Mo (VI)-ICTGB, the gel beads after adsorbing Mo (VI) ions in Fig. 2f become flat relatively, and a lot of tiny particles appear on its surface.

Some parameters of Mo (VI)-ICTGBs and NICTGBs obtained by BET model and BJH formula were shown in Table S2 (Supporting Information). Compared with NICTGBs, Mo (VI)-ICTGBs increase obviously in specific surface area and total pore volume. The increase of pore volume in Mo (VI)-ICTGBs is due to the cavities resulted by eluting Mo (VI) ion from CTMoBs, which suggest that the increase of adsorption capacity in Mo (VI)-ICTGBs is owe to the increase of specific surface area.

3.4. XRD analysis

Two characteristic peaks of the raw CTS material at 2θ= 10° and 2θ=20° and a shoulder close to 2θ=21°(Dambies et al., 2001; Ding et al., 2006). For the CTS beads obtained in the mixed coagulating bath containing sodium hydroxide and molybdate, the peaks is much reduced at 2θ=10°, 20° (Fig. 3b). However, the two peaks increase obviously in intensity after eluting Mo (VI) in Fig. 3a. These results are corresponding to the results obtained by Dambies et al. (2001). Dambies et al. (2001) also confirmed that the decrease in the crystallinity of the sorbent follows the variation: Raw CTS > CTS dissolved and precipitated in NaOH > CTS coagulated in molybdate solution. XRD pattern of CTMoB obtained in the mixed coagulating bath with TEA in place of NaOH shows that the peak at 2θ=10° disappears, which is attributed to the deformation of the CTS backbone chain as TEA are involved in forming gel beads. Furthermore, the peak at 2θ = 10° has not reappeared after removing Mo(VI), which implies that TEA has still important effect on the structure of the Mo(VI)-ICTGB.

3.5. Effect of pH on adsorption capacity

pH value is one of the most important parameters governing the uptake of metal ions on CTS and the distribution of molybdate ion species (Zhao & Yu, 2007; Dambies et al., 2001). The pH of best suitable adsorption is about 6.0 (The data is shown in Fig. S3, Supporting Information). When pH > 4.5 in adsorption solution, the major species are $HMoO_4^-$ and MoO_4^{2-} (Dambies et al., 2001). Therefore, the main adsorption species is $MoO4^{2-}$ in this work. Moreover, the pH 6.0 is in agreement with the pH of mixed coagulation bath. This also indicates the specific of imprinted materials to object ion. At pH > 6.0, adsorption capacity of molybdate decreases. This could be attributed to electrostatic repulsion between the negatively charged adsorbent surface and the molybdate anions. This suggested that chemisorption might be involved in the adsorption process (Namasivayam & Sangeetha, 2006). At pH < 6.0, adsorption capacity of molybdate decreases with the reduction of pH because

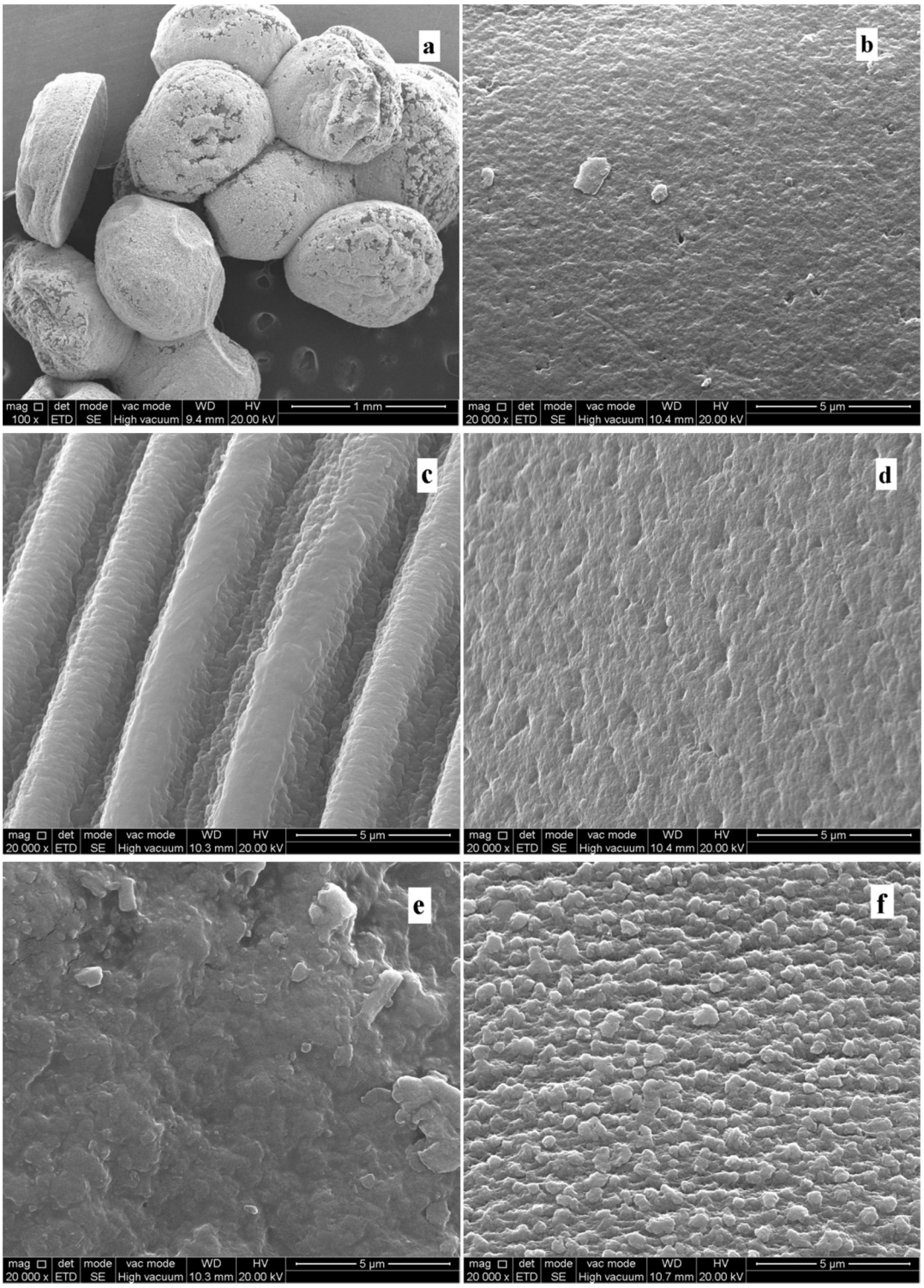

Fig. 2. Surface appearance of (a), Mo(VI)-ICTGBs (100 ×); (b), NICTGB (20,000 ×); (c), CMoB (20,000 ×); (d), CTMoB (20,000 ×); (e), Mo(VI)-ICTGB (20,000 ×); (f), Mo(VI)-ICTGB after adsorption (20,000 ×).

molybdate ion species in solution are incompatible with Mo (VI)-ICTGBs.

3.6. Adsorption isotherm

Static equilibrium test was carried out to study the isothermal adsorption of Mo (VI)-ICTGB. In Fig. 4, it was shown that the adsorption capacity increased with growing the equilibrium concentration of Mo (VI) until it reached saturation. The Langmuir and Freundlich models are commonly used to fit experimental data when solute uptake occurs by a monolayer sorption (Dambies et al., 2001). The two models were tested in the present work, but Langmuir model did not exhibit good fit to the sorption data (The data is shown in Fig. S4, Supporting Information). The results in Fig. 4 were fitted in the following Freundlich model (Vold et al., 2003).

$$Q_e = k_f \times c_e^{1/n} \quad (4)$$

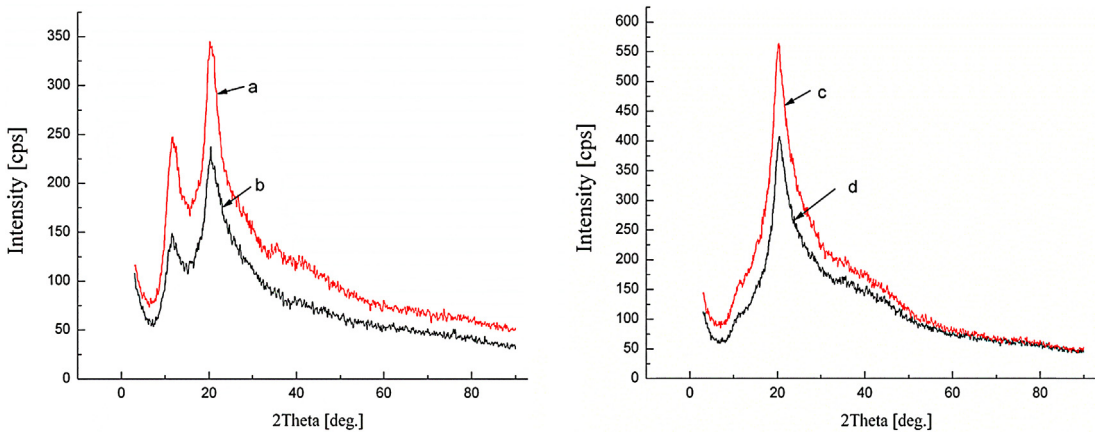

Fig. 3. XRD patterns of (a), CTS/NaOH/Mo (VI) beads after eluting Mo (VI);(b), CTS/NaOH/Mo(VI) gel beads;(c), Mo (VI)-ICTGB;(d), CTMoB.

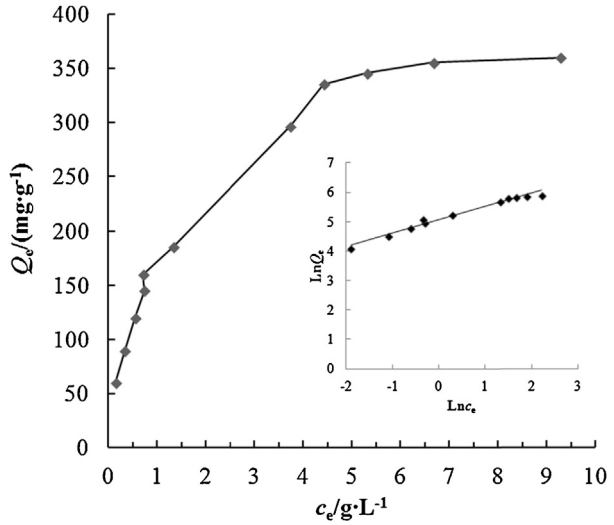

Fig. 4. Relationship of the equilibrium adsorption concentration and equilibrium adsorption capacity on Mo(VI).

Where k_f and n are the capacity ($g^{-1}\,L^{1/n}\,mg^{1-1/n}$) and the intensity constants, respectively. Fig. 4 also shows the fitted equilibrium data in Freundlich isotherm expressions for Mo (VI)-ICTGB. The correlation coefficient (r^2) is 0.990 for Mo (VI)-ICTGB, which show that the Freundlich adsorption model can be applied in this affinity adsorbent system. The values of k_f and n can be calculated to be 199.0 and 2.45 from the intercept and slope of the linear plot of $\ln Q_e$ against $\ln c_e$, respectively. It appears that the isothermal adsorption of Mo (VI)-ICTGB is based on an exponential distribution of sorption sites and energies. Moreover, the molecules adsorbed on the surface can interact.

3.7. Adsorption kinetics

The kinetics of adsorption that describes the solute uptake rate governing the contact time of the sorption reaction is one of the important characteristics that define the efficiency of sorption. Mo (VI) solution ($8.000\,g\,L^{-1}$) were prepared for adsorption testing of Mo (VI)-ICTGBs and NICTGBs. Fig. 5a shows that adsorption capacity increased with growing time until it reached adsorption equilibrium. It reached equilibrium at 600 min for Mo (VI)-ICTGBs. Compared with Mo (VI)-ICTGBs, NICTGBs is smaller in adsorption capacity, which is because NICTGBs does not contain the cavities matching with Mo (VI) in structure and dimension. In order to investigate the mechanism of adsorption kinetics for Mo (VI)-ICTGBs, the following kinetic models were tested to interpret data obtained from batch experiments (Ho & McKay, 1998).

$$lg(Q_e - Q_t) = lgQ_e - \frac{k_1 t}{2.303} \tag{5}$$

$$\frac{t}{Q_t} = \frac{t}{Q_e} + \frac{1}{k_2 Q_e^2} \tag{6}$$

The data in Fig. 5a were fitted by Eqs. (5), (6), and the results were shown in Fig. 5b and Fig. 5c. When the experimental data were plotted in form of log ($Q_e - Q_t$) versus t, a straight line would be obtained if the pseudo-first order kinetic model is a suitable expression. The rate constant (k_1) can be obtained from the slope of the line. The pseudo-second order rate equation could be applied if the adsorption capacity of adsorbent is proportional to the number of active sites on its surface. The values of k_2 (slope^2/intercept), Q_e (1/slope) can be determined graphically from the slope and intercept of the revealed plots by plotting t/Q_t against t.

The adsorption kinetic constants and linear regression values were summarized in Table 1. As seen in Table 1, the calculated Q_e ($500\,mg\,g^{-1}$) value estimated from pseudo-second order kinetic model was very close to the experimental value ($458\,mg\,g^{-1}$) and also the correlation coefficients for the second order kinetic plots at all the studied concentrations were above 0.994. The results suggest that the pseudo-second order adsorption mechanism was predominant for this adsorbent system of Mo (VI)-ICTGBs (Namasivayam & Sangeetha, 2006).

Table 1
Kinetic parameters of the pseudo-order for Mo(VI)adsorption on Mo(VI)-ICTGBs.

	Q_e(exp)/(mg g^{-1})	Pseudo-first order			Pseudo-second order		
		k_1/min^{-1}	Q_e/(mg g^{-1})	r^2	k_2/min^{-1}	Q_e/(mg g^{-1})	r^2
Mo(VI)-IICB	458	0.00484	375	0.911	2.01×10^{-5}	500	0.994

Table 2
Selective absorption properties of Mo (VI)-ICTGBs and NICTGBs.

Substrate	$Q/(mg\,g^{-1})$		$K_d/(mL\,g^{-1})$		k	
	Mo (VI)-ICTGBs	NICTGBs	Mo (VI)-ICTGBs	NICTGBs	Mo (VI)-ICTGBs	NICTGBs
Mo(VI)	37.04	18.1	1430.0	283.7	–	–
V(VI)	30.61	15.2	894.9	227.2	1.60	1.34
Cr (VI)	19.00	12.2	291.1	159.4	4.91	1.78
As (VI)	16.00	13.0	235.3	175.8	6.08	1.74

Different adsorbents in adsorption for Mo (VI) ions reported in the literature were listed in Table S1 (Seen in Supporting Information). Compared with these adsorbents, Mo (VI)-ICTGBs show advantage in Q (Capacity) value for the adsorption of Mo (VI) ions besides crosslinking chitosan flakes. However, the crosslinking chitosan flakes is poor in reusability as adsorbent.

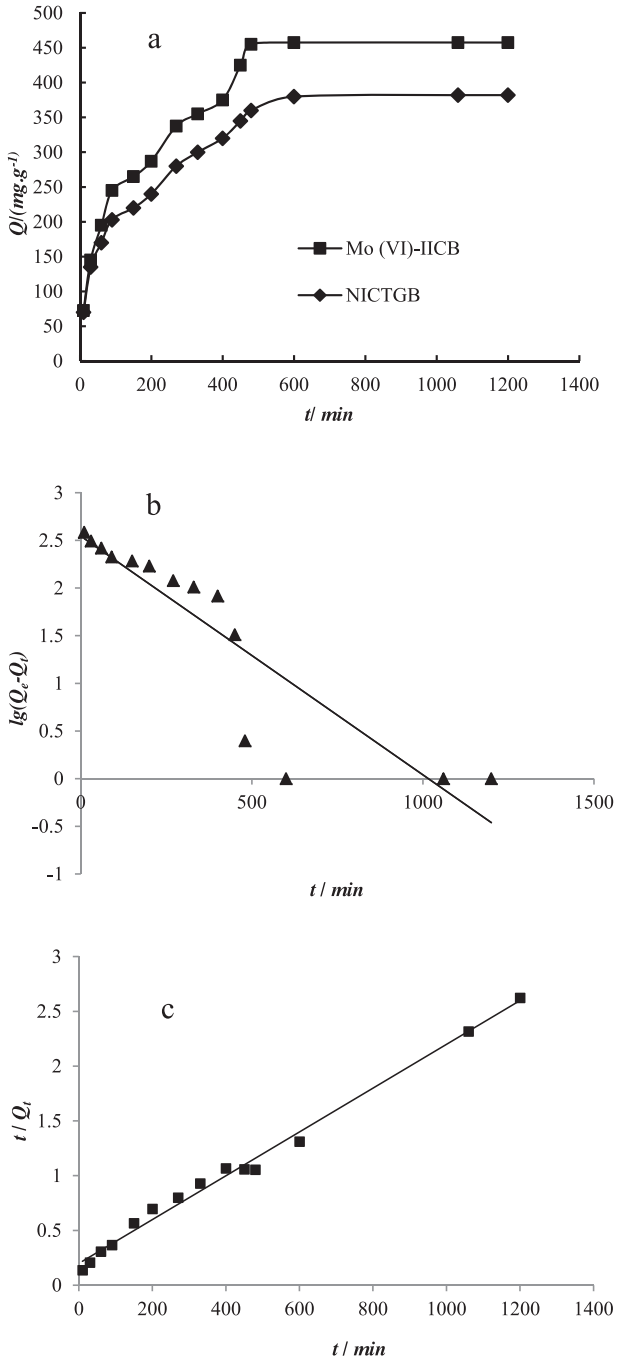

Fig. 5. Adsorption kinetics curve of (a), Mo (VI)-IICBs and NICTGBs; linear plot of (b), $\log(Q_e - Q_t)$ vs. t; (c), t/Q_t vs. t for Mo (VI)-IICBs, $C_0 = 8.0\,g\,L^{-1}$.

3.8. Adsorption selectivity of Mo (VI)-IICBs

Molybdate waste water contains a lot of nitrate ion. In addition, there are also some Fe^{3+} and a few other cations. The study indicates that CTS shows strong selectivity for binding of molybdate when there are molybdate, chloride and nitrate in the system of solution (Muzzarelli & Rocchetti, 1973; Vold et al., 2003). In addition, our study also found that Fe^{3+} ions have no effect on the adsorption of Mo (VI) ion. Therefore, the mixed solution containing molybdate, chromate, vanadate and arsenate was used to perform a study of competitive adsorption in this work. The results in Table 2 show that the Mo (VI)-ICTGBs had high adsorption capacity and good selectivity for Mo (VI) anions in the coexistence system at pH = 6.0, compared with the results obtained from Muzzarelli and Rocchetti, (1973). But because V (VI) ion is similar to Mo (VI) ion in radius and structure, the adsorption for V (VI) ion is more than two other anions. Compared with Mo (VI)-ICTGBs, NICTGBs for all of ions are poor in adsorption capacity and selective absorption for Mo (VI) ion.

3.9. Column Adsorption

Adsorption breakthrough curve for Mo (VI) ions on Mo (VI)-ICTGBs at 25 °C and pH = 6.0 are shown in Fig. 6. As can be seen, a few Mo (VI) ions were found in the effluent up to 20 bed volumes, and then the concentration of Mo (VI) ions increases slowly, as a consequence of the progressive saturation of the binding sites. In practice, Mo (VI) ions (<100 mg L^{-1}) in wastewater could be recovered with column thoroughly within 20BV.

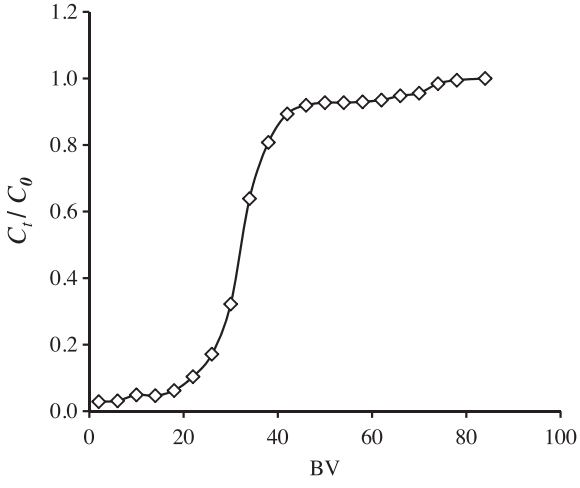

Fig. 6. Column break-through curve for adsorption of Mo (VI) on Mo (VI)-ICTGB.

3.10. Elution and regeneration cycles

Ten cycle runs on adsorption/desorption were carried out for Mo (VI) on Mo (VI)-ICTGBs. Sodium hydroxide solution (8.0 g L^{-1}) was used for elution. The material showed no appreciable changes in adsorption capacity during successive cycles up to 10 times (250 mg g^{-1} < Q < 300 mg g^{-1}, the data is shown in Fig. S5, Supporting Information). Compared with Mo (VI)-ICTGBs, CMoBs prepared without TEA in the mixed coagulation bath became powder after one cycle run. In addition, compared with the adsorbents shown in Table S1 (Seen in Supporting Information), the Mo (VI)-ICTGBs have good durability and good efficiency for repeated use. The Mo (VI)-ICTGBs were used for molybdate wastewater by batch adsorption (the initial Mo (VI) anion is 1.000 g L^{-1}). The equilibrium concentration is 0.500 g L^{-1} after adsorption, and the adsorption capacity is up to 120 mg g^{-1}, which is closed to the value number obtained by static equilibrium test. When the above solution was diluted to 100 mg L^{-1}, the recovery rate is over 95% with the above column.

4. Conclusions

The Mo (VI)-ICTGBs were prepared by ionic gel reaction between molybdate and CTS, and TEA was used as crosslinking agent. The process of preparing Mo (VI)-ICTGBs is simple and rapid. The pH value of the mixed coagulation bath is about 6.0, so main species of molybdate is MoO_4^{2-}. Moreover, the adsorption experiment results also indicate that the best adsorption condition of pH is also about 6.0, which shows good selectivity for MoO_4^{2-}. SEM prove that surface area of Mo (VI)-ICTGB increase comparing to CTMoB; FT-IR spectrum show that there are hydrogen bond and ion gel reaction among TEA, CTS and molybdate; XRD show that the structure of CTMoB is different from CTS/NaOH/Mo (VI) gel beads. The above methods prove that the process of preparing Mo (VI)-ICTGB is reasonable by ion imprinted technology. Static equilibrium test show that the adsorption of Mo (VI)-ICTGBs for Mo (VI) is in agreement with Freundlich models. The kinetics of adsorption studies imply that the control process is corresponding to pseudo-second order kinetic model. The research on repeated application show good durance and the results on removing Mo (VI) in wastewater show the similar effect as static equilibrium test. The Mo (VI)-ICTGBs are easy to manufacture, convenience to apply in separation and concentration, and have a good application prospect.

Acknowledgments

The authors are grateful to partial support from the National Science Foundation of China (51278407) and the Project Supported by Natural Science Basic Research Plan in Shaanxi Province of China (Program No. 2012JZ7003).

Appendix A. Supplementary data

Supplementary material related to this article can be found, in the online version, at http://dx.doi.org/10.1016/j.carbpol.2014.08.049.

References

Afkhami, A., & Conway, B. E. (2002). Investigation of removal of Cr(VI), Mo(VI), W(VI), V(IV), and V(V) oxy-ions from industrial waste-waters by adsorption and electrosorption at high-area carbon cloth. *Journal of Colloid and Interface Science*, *251*, 248–255.

Antelo, J., Fiol, S., Gondar, D., López, R., & Arce, F. (2012). Comparison of arsenate, chromate and molybdate binding on schwertmannite: Surface adsorption vs anion-exchange. *Journal of Colloid and Interface Science*, *386*(1), 338–343.

Asem, A. A., Ahmed, M. D., & Haytham, A. A. (2008). Synthesis of magnetic chelating resins functionalized with tetraethylenepentamine for adsorption of molybdate anions from aqueous solutions. *Journal of Hazardous Materials*, *155*, 100–108.

Atia, A. A. (2008). Adsorption of chromate and molybdate by cetylpyridinium bentonite. *Applied Clay Science*, *41*, 73–84.

Chassary, P., Vincent, T., & Guibal, E. (2004). Metal anion sorption on chitosan and derivative materials: A strategy for polymer modification and optimum use. *Reactive & Functional Polymers*, *60*, 137–149.

Chen, C. Y., Chang, T. H., Kuo, J. T., Chen, Y. F., & Chu, Y. C. (2008). Characteristics of molybdate-impregnated chitosan beads (MICB) in terms of arsenic removal from water and the application of a MICB-packed column to remove arsenic from wastewater. *Bioresource Technology*, *99*, 7487–7494.

Dambies, L., Vincent, T., Domard, A., & Guibal, E. (2001). Preparation of chitosan gel beads by ionotropic molybdate gelation. *Biomacromolecules*, 1198–1205.

Dambies, L., Vincent, T., & Guibal, E. (2002). Treatment of arsenic-containing solutions using chitosan derivatives: Uptake mechanism and sorption performances. *Water Research*, *36*, 3699–3710.

Ding, S. M., Zhang, X. Y., Feng, X. H., Wang, Y. T., Ma, S. L., Peng, Q., et al. (2006). Synthesis of *N,N′*-diallyl dibenzo 18-crown-6 crown ether crosslinked chitosan and their adsorption properties for metal ions. *Reactive & Functional Polymers*, *66*, 357–363.

Draget, K. I., Värum, K. M., Moen, E., Gynnild, H., & Smidsrød, O. (1992). Chitosan cross-linked with Mo(VI) polyoxyanions: A new gelling system. *Biomaterials*, *13*(9), 635–638.

Fei, X., Zhang, L., Zhong, L. l., Chen, S. l., & Ma, C. l. (2012). Preparation of chitosan gel beads imprinting anion Mo(VI). *Youse Jinshu Yelian Bufen (Chinese)*, (2), 50–53.

Guibal, E., Milot, C., & Tobin, J. M. (1998). Metal-anion sorption by chitosan beads: Equilibrium and kinetic studies. *Industrial & Engineering Chemistry Research*, *37*, 1454–1463.

Guibal, E., Milot, C., Eterradoss, O., Gauffier, C., & Domard, A. (1999). Study of molybdate ion sorption on chitosan gel beads by different spectrometric analyses. *International Journal of Biological Macromolecules*, *24*, 49–59.

Guibal, E., Milot, C., & Roussy, J. (2000). Influence of hydrolysis mechanisms on molybdate sorption isotherms using chitosan. *Separation Science and Technology*, *35*(7), 1021–1038.

Ho, Y. S., & McKay, G. (1998). Kinetic models for the sorption of dye from aqueous solution by wood. *Transactions of the American Institute of Chemical Engineers*, *76B*, 183–191.

Lee, S. T., Mi, F. L., Shen, Y. J., & Shyu, S. S. (2001). Equilibrium and kinetic studies of copper (II) ion uptake by chitosan-tripolyphosphate chelating resin. *Polymer*, *42*, 1879–1892.

Muzzarelli, R. A. A., & Rocchetti, R. (1973). The determination of molybdenum in sea water by hot graphite atomic absorption spectrometry after concentration on p-aminobenzyl cellulose or chitosan. *Analytica Chimica Acta*, *64*, 371–379.

Muzzarelli, R. A. A. (2011). Potential of chitin/chitosan-bearing materials for uranium recovery: An interdisciplinary review. *Carbohydrate Polymers*, *84*, 54–63.

Namasivayam, C., & Sangeetha, D. (2006). Removal of molybdate from water by adsorption onto $ZnCl_2$ activated coir pith carbon. *Bioresource Technology*, *97*, 1194–1200.

Naja, G., & Volesky, B. (2011). The mechanism of metal cation and anion biosorption. *Microbial Biosorption of Metals*, *11*, 19–58.

Rojas, G., Silva, J., Flores, J. A., Rodriguez, A., Ly, M., & Maldonado, H. (2005). Adsorption of chromium onto cross-linked chitosan. *Separation and Purification Technology*, *44*, 31–36.

Ren, Y. M., Wei, X. Z., & Zhang, M. L. (2008). Adsorption character for removal Cu(II) by magnetic Cu(II) ion, imprinted composite adsorbent. *Journal of Hazardous Materials*, *158*, 14–22.

Ren, Y. M., Liu, P. X., Feng, J., Ma, J., Wen, Q., & Zhang, M. L. (2013). Selective recognition of molybdenum(VI) from water by Mo(VI) oxy ion-imprinted particle as an adsorbent. *Chemical Engineering Journal*, *219*, 286–294.

Varma, A. J., Deshpande, S. V., & Kennedy, J. F. (2004). Metal complexation by chitosan andits derivatives: A review. *Carbohydrate Polymers*, *55*, 77–93.

Vold, I. M. N., Vårum, K. M., Guibal, E., & Smidsrød, O. (2003). Binding of ions to chitosan—selectivity studies. *Carbohydrate Polymers*, *54*, 471–477.

Wei, D. W., Sun, W. Y., Qian, W. P., Ye, Y. Z., & Ma, X. Y. (2009). The synthesis of chitosan-based silver nanoparticles and their antibacterial activity. *Carbohydrate Research*, *344*, 2375–2382.

Xu, N. C. C., & Washington, B. (2006). Modeling the competitive effect of phosphate, sulfate, silicate, and tungstate anions on the adsorption of molybdate onto goethite. *Chemosphere*, *64*, 1325–1333.

Zhang, L., Yang, S. W., Han, T., Zhong, L. L., Ma, C. L., Zhou, Y. Z., et al. (2012). Improvement of Ag(I) adsorption onto chitosan/triethanolamine compositesorbent by an ion-imprinted technology. *Applied Surface Science*, *263*, 696–703.

Zhao, F., & Yu, B. Y. (2007). Preparation of porous chitosan gel beads for copper(II) ion adsorption. *Journal of Hazardous Materials*, *147*, 67–73.